Journal of Control, Automation and Electrical Systems (2018) 29:558–565
https://doi.org/10.1007/s40313-018-0409-4

Control with Sensor Fault Tolerance for an Underactuated Linear Positioning System Using the TFL/LTR Technique

Emilio Tanowe Maddalena[1] · **Karl Heinz Kienitz**[1]

Received: 6 February 2018 / Revised: 11 June 2018 / Accepted: 8 August 2018 / Published online: 14 August 2018

Abstract
In this work, the applicability of a Lyapunov filter-based target feedback loop/loop transfer recovery controller to open-loop unstable plants is investigated on an underactuated linear positioning mechanism. Uncertainties in friction coefficients are taken into account. Lyapunov filter target loops yield robustly stable dynamics and tolerance to abrupt sensor faults, i.e., sensors affected by any attenuation in the interval [0, 1). Experimental results confirm the effectiveness of the proposed solution when compared to alternative control methods.

Keywords Robust control · TFL/LTR controllers · Fault tolerance · Underactuated systems

1 Introduction

Doyle's paper Doyle (1978) is considered a watershed for the robust control field since it demonstrated how fragile observer-based controllers can be when not designed properly. This sparked in the research community a will to improve the robustness properties of observer-based compensators. One well-known method to overcome this limitation is the linear quadratic gaussian/loop transfer recovery (LQG/LTR) procedure, where the filter gain is modified by manipulating certain weight matrices. At the expense of losing estimator optimality in the sense of minimum variance, the desirable gain and phase margins of the linear quadratic regulator (LQR) can be asymptotically recovered (Athans 1986; Stein and Athans 1987; Skogestad and Postlethwaite 2001). The concept of LTR was formulated by Doyle and Stein in a series of papers (Doyle and Stein 1979, 1981) mainly exploring ideas published earlier in Kwakernaak (1969). Subsequently, the original procedure was extended to discrete-time (Maciejowski 1985; Saberi et al. 1993) and non-minimum phase systems (Zhang and Freudenberg 1990; Saberi et al. 1991a, b). In Prakash (1990a, b), Prakash studied the applicability of several alternative target loops including structures presented in Lehtomaki et al. (1981) and coined the term target feedback loop/loop transfer recovery (TFL/LTR), which encompasses the LQG/LTR as a particular case. The main appeal of the TFL/LTR technique is the possibility of employing structures with larger guaranteed stability margins than those of the LQR. Although many results in the LTR field were developed in the 1980s and 1990s, the topic was revitalized in recent years by authors who presented important new contributions, addressing bilinear systems (Chen and Chen 2008), disturbance cancelation (Ishihara and Guo 2008), $\mathcal{H}_\infty$/LTR control (Paula and Ferreira 2011; Silva et al. 2014; Guaracy et al. 2015a), adaptation mechanisms based on LTR (Calise and Yucelen 2012; Lavretsky 2012; George 2014), retrieving performance in terms of the original cost functions (Ravanbod et al. 2012), and obtaining target loops with decoupled channels (Guaracy et al. 2015b).

Besides the aforementioned theoretical advances, LQG/LTR has been utilized in several application fields such as temperature control of nuclear reactors (Arab-Alibeik and Setayeshi 2003), space launchers and aircraft stabilization (Abbas-Turki et al. 2007; Zarei et al. 2007), oscillations damping in power systems (Zolotas et al. 2007), doubly fed induction motors speed regulation (Pinto et al. 2011), and water level control in industrial tanks (Moraes and Kienitz 2017). In safety critical applications it is crucial to systematically account for possible component faults still in the design phase, thus producing fault-tolerant control systems (FTCS) (Alwi et al. 2011). A reconfigurable FTCS based on

✉ Emilio Tanowe Maddalena
tanowe@ita.br

Karl Heinz Kienitz
kienitz@ita.br

[1] Divisão de Engenharia Eletrônica, Insituto Tecnológico de Aeronáutica, São José dos Campos, SP 12228-900, Brazil

loop recovery is presented in Niemann and Stoustrup (2003), where the controller parameters are left unchanged and only the state observer is modified. In Prakash (1990a, b), two structures named linear Lyapunov regulator (LLR) and Lyapunov filter (LF) capable of tolerating faults in the input and output channels, respectively, were introduced. More specifically, abrupt arbitrary attenuations can independently occur on every input or output channel without compromising the closed-loop system stability. Nevertheless, these structures require all poles of the system to be located in the open left half-plane (OLHP). Prakash reported a case study on the control of an induction motor using a LF-based TFL/LTR design in Prakash (1992), but did not consider any sensor fault. Moreover, the induction motor model was rather simple, being single-input single-output (SISO) and open-loop stable. Hence, the full potential of the Lyapunov filter was not exploited.

In this paper, the applicability of a Lyapunov filter-based TFL/LTR controller to an underactuated linear positioning system with one input and two outputs is investigated. Uncertainties are taken into account in the friction coefficients between the masses and the steel shaft on which they slide. An internal feedback loop is used to pre-stabilize the system and comply with the Lyapunov filter restrictions, while the outer TFL/LTR controller assures performance and tolerance to parasitic abrupt attenuations on the remaining output channel. As opposed to Niemann and Stoustrup (2003), the fault-tolerant attribute of the proposed solution is based on the controller inherent multivariable gain margins and, thus, it does not require any fault detection and diagnosis (FDD) mechanism. Despite being passive, the presented approach is shown to yield similar performance to another control method that requires measuring all states. The main contribution of this work is to elucidate how the Lyapunov filter (and, by analogy, the linear Lyapunov regulator) can be applied to open-loop unstable systems. Moreover, a necessary condition to dispense with the need of implementing the internal control loop is given. A preliminary version of this work was presented in Maddalena and Kienitz (2017). The reminder of this work is organized as follows. In Sect. 2, the plant dynamic equations and associated uncertainties are covered. The design requirements and the proposed TFL/LTR controller are presented in Sect. 3. Experimental results in normal operation and under sensor fault are given in Sect. 4, followed by the concluding remarks in Sect. 5.

Notation: The set of real numbers is denoted by $\mathbb{R}$. $G(s)$ is the plant nominal model transfer function matrix, whereas $K(s)$ is the controller transfer function matrix. Ω is the set of dynamic models arising from the nominal model uncertainties. The loop transfer function, sensitivity and complementary sensitivity are denoted, respectively, by $L(s) \triangleq G(s)K(s)$, $S(s) \triangleq (I + G(s)K(s))^{-1}$ and $T(s) \triangleq G(s)K(s)(I + G(s)K(s))^{-1}$. The maximum and minimum singular values are represented by $\overline{\sigma}(\cdot)$ and $\underline{\sigma}(\cdot)$. The symbols $||\cdot||$ and $||\cdot||_\infty$ denote the Euclidean norm of a vector and the H-infinity norm of a transfer function matrix, respectively. Finally, given a matrix M, M^T represents its transpose, while $M \succ 0$ ($M \succeq 0$) indicates that M is positive definite (positive semidefinite).

2 System Description

2.1 Mathematical Model

The linear positioning system is depicted in Fig. 1. It consists of an active cart, which is driven by a direct-current (DC) motor, connected to a passive cart through a linear spring. Both masses slide on a stainless steel shaft and are equipped with 0.023 mm resolution encoders. The whole setup is connected to a desktop computer through an USB module and a power amplifier, which sends the feedback signals to the computer and drive the DC motor actuator.

The state vector $x_o = \begin{bmatrix} x_{\mathrm{ac}} & x_{\mathrm{pc}} & \dot{x}_{\mathrm{ac}} & \dot{x}_{\mathrm{pc}} \end{bmatrix}^T$ contains the active cart position x_{ac}, the passive cart position x_{pc}, the active cart velocity $\dot{x}_{\mathrm{ac}}$ and the passive cart velocity $\dot{x}_{\mathrm{pc}}$. The input $u(t)$ is the voltage applied to the DC motor, which is bounded to $[-6, +6]$ V according to the limits specified by the manufacturer. Approximating dry friction by viscous friction, the obtained dynamics are (Quanser Consulting 2012)

$$\dot{x}_o(t) = A_o x_o(t) + B_o u(t) \tag{1}$$

$$A_o = \begin{bmatrix} 0 & 0 & 1 & 0 \\ 0 & 0 & 0 & 1 \\ -\frac{K_{\mathrm{s}}}{m_{\mathrm{ac}}} & \frac{K_{\mathrm{s}}}{m_{\mathrm{ac}}} & \frac{b_{\mathrm{ac}} + \frac{K_{\mathrm{g}}^2 K_{\mathrm{m}} K_{\mathrm{t}}}{R_{\mathrm{m}} R_{\mathrm{mp}}^2}}{m_{\mathrm{ac}}} & 0 \\ \frac{K_{\mathrm{s}}}{m_{\mathrm{pc}}} & -\frac{K_{\mathrm{s}}}{m_{\mathrm{pc}}} & 0 & -\frac{b_{\mathrm{pc}}}{m_{\mathrm{pc}}} \end{bmatrix} \tag{2}$$

$$B_o = \begin{bmatrix} 0 & 0 & \frac{K_{\mathrm{g}} K_{\mathrm{t}}}{R_{\mathrm{m}} r_{\mathrm{mp}}} & 0 \end{bmatrix}^T \tag{3}$$

where the description and value of each parameter are given in Table 1. For convenience, a change of variables is proposed to describe the system with a different state vector $x \triangleq \begin{bmatrix} x_{\mathrm{ac}} & (x_{\mathrm{ac}} - x_{\mathrm{pc}}) & \dot{x}_{\mathrm{ac}} & (\dot{x}_{\mathrm{ac}} - \dot{x}_{\mathrm{pc}}) \end{bmatrix}^T$. In this new frame of reference, $(x_{\mathrm{ac}} - x_{\mathrm{pc}})$ is the difference between the active

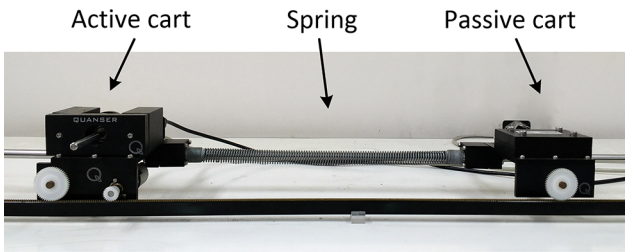

Fig. 1 The underactuated linear positioning system

Table 1 Physical system parameters

Parameter	Description	Value
K_s	Spring stiffness coefficient	142 N/m
m_{ac}	Active cart mass	1.15 kg
m_{pc}	Passive cart mass	0.54 kg
b_{ac}	Active cart friction coefficient	5.4 Ns/m
b_{pc}	Passive cart friction coefficient	2.2 Ns/m
K_g	Gearbox ratio	3.71
K_m	Force constant	7.67×10^{-3} Vs/rad
K_t	Motor torque constant	7.67×10^{-3} Nm/A
R_m	Motor armature resistance	2.6 Ω
R_{mp}	Motor pinion radius	6.35×10^{-3} m

and passive cart positions, while $(\dot{x}_{ac} - \dot{x}_{pc})$ is the difference between the active and passive cart velocities. This is accomplished by the similarity transform

$$M = \begin{bmatrix} 1 & 0 & 0 & 0 \\ 1 & -1 & 0 & 0 \\ 0 & 0 & 1 & 0 \\ 0 & 0 & 1 & -1 \end{bmatrix} \tag{4}$$

with $x = Mx_o$, $A_n = MA_oM^{-1}$, $B_n = MB_o$ and $\dot{x}(t) = A_n x(t) + B_n u(t)$. The system outputs are defined as $y = \begin{bmatrix} x_{ac} & (x_{ac} - x_{pc}) \end{bmatrix}^T$. It should be noted that the second output $(x_{ac} - x_{pc})$ is equivalent to the spring deformation; indeed, the spring will be compressed if $(x_{ac} - x_{pc}) > 0$ and elongated if $(x_{ac} - x_{pc}) < 0$.

Substituting the numerical values into the state matrix A_o, its eigenvalues are found to be $-3.66 \pm j20.54$, -11.31 and 0. Due to the pole at the origin, there is a violation of the Lyapunov Filter requirements. To overcome this limitation, the active cart position sensor is used to build an internal feedback loop and shift this specific pole into the OLHP. Clearly, the main drawback of this approach is the insertion of steady-state error, which was not present in the original system. Minimizing this side effect is possible if a low feedback gain ϵ is used (Maddalena 2017)

$$\dot{x}(t) = \overbrace{(A_n - B_n K)}^{A} x(t) + \overbrace{B_n}^{B} u(t) \tag{5}$$

$$y(t) = C\,x(t) \tag{6}$$

where $K = \begin{bmatrix} \epsilon & 0 & 0 & 0 \end{bmatrix}$. Setting $\epsilon = 0.1$ and substituting all numerical values in (5) and (6) we obtain

$$A = \begin{bmatrix} 0 & 0 & 1 & 0 \\ 0 & 0 & 0 & 1 \\ -0.1724 & -151.0638 & -13.9612 & 0 \\ -0.1724 & -453.1915 & -9.2804 & -4.6809 \end{bmatrix} \tag{7}$$

$$B = \begin{bmatrix} 0 & 0 & 1.7235 & 1.7235 \end{bmatrix}^T \tag{8}$$

$$C = \begin{bmatrix} 1 & 0 & 0 & 0 \\ 0 & 1 & 0 & 0 \end{bmatrix}. \tag{9}$$

The above system has no zeros and poles located at $-3.67 \pm j20.55$, -11.29 and -0.01; hence, matrix A is Hurwitz. Moreover, it is also fully controllable and observable.

2.2 Plant Uncertainties

Simplifying the modeling process by assuming viscous friction was necessary to obtain a linear model of the positioning system. Nevertheless, the nonlinear nature of dry friction may cause the real mechanical behavior to deviate from the model response (Urbakh et al. 2004). Therefore, b_{ac} and b_{pc} were considered to be uncertain parameters.

The unstructured output multiplicative form was chosen to represent the plant uncertainties (Skogestad and Postlethwaite 2001), yielding a family Ω of dynamic models

$$\Omega = \{G'(s) | G'(s) = [I + \Delta(s) w_O(j\omega)]\, G(s), \ldots \\ \ldots ||\Delta(s)||_\infty \leq 1\} \tag{10}$$

where $G'(s)$ is a possible plant transfer function, $G(s)$ is the nominal transfer function, $\Delta(s)$ are unknown complex perturbations, and $w_O(\omega)$ is the uncertainty weight. A total variation of ± 30% on the viscous friction coefficients b_{ac} and b_{pc} was taken into account in steps of 5%. For all 36 possible coefficient combinations, the perturbed transfer function $G_P(s)$ was computed to generate the uncertainty functions $(G_P(s) - G(s))G^*(s)$, where $G^*(s)$ denotes the pseudoinverse of $G(s)$ (Skogestad and Postlethwaite 2001). Figure 2 presents the obtained singular values and the chosen upper bound for the modeling error

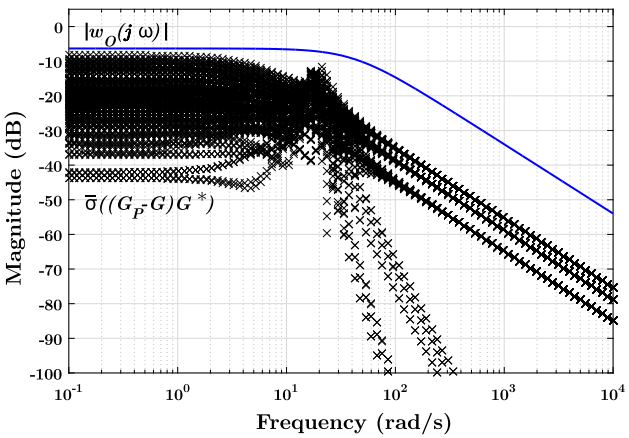

Fig. 2 Output multiplicative error for all possible friction coefficient scenarios and constructed uncertainty weight

$$w_O(j\omega) = \frac{13}{j\omega + 41.43}. \tag{11}$$

3 Controller Design

The design requirements for the closed-loop system are good reference tracking for the active cart position while maintaining the spring deformation close to zero as much as possible. No saturation of the control signal is tolerated since nonlinear effects are to be avoided. Stability must be ensured not only for the nominal plant $G(s)$, but also for the entire Ω set. Moreover, abrupt parasitic attenuations in the spring deformation feedback signal must not destabilize the system. Lastly, the following high-frequency barriers must be avoided to assure sensor noise rejection (see da Cruz 1996 for further details)

barrier 1:

$$\overline{\sigma}(L(j\omega)) \leq \frac{0.05}{1 + |w_O(j\omega)|}, \ \omega > 10^2 \text{ rad/s} \tag{12}$$

barrier 2:

$$\overline{\sigma}(L(j\omega)) \leq \frac{0.005}{1 + |w_O(j\omega)|}, \ \omega > 10^3 \text{ rad/s}. \tag{13}$$

3.1 Target Feedback Loop Design

Definition 1 Saberi et al. (1993): Given a linear system Σ described by the triple $\{A, B, C\}$, $A \in \mathbb{R}^{n\times n}$, $B \in \mathbb{R}^{n\times p}$, $C \in \mathbb{R}^{q\times n}$, the set of admissible target loop transfer functions for perturbations reflected to output (PRO) designs is defined by

$$\begin{aligned} T(\Sigma) = &\{L_T(s) \mid L_T(s) = C\Phi K_f, \ldots \\ &\ldots \ (A - K_f C) \ Hurwitz\} \end{aligned} \tag{14}$$

where $\Phi \triangleq (sI - A)^{-1}$ and $K_f \in \mathbb{R}^{n\times q}$ is the filter gain.

In the sequel, we describe the process of calculating the gain K_f using the LF procedure proposed in Prakash (1990b). Given a system Σ with all eigenvalues of A in the OLHP, and $Q \in \mathbb{R}^{n\times n}$, $Q \succeq 0$, the equation

$$AP + PA^T + Q = 0 \tag{15}$$

is solved for $P \in \mathbb{R}^{n\times n}$. Consider now $R \in \mathbb{R}^{q\times q}$, $R \succ 0$, the Lyapunov Filter is then a gain given by

$$K_f = PC^T R^{-1}. \tag{16}$$

Theorem 1 Prakash (1990a, b): *If the Lyapunov Filter is designed with $Q \succ 0$, and $R \succ 0$ diagonal, the guaranteed multivariable gain margins (GGM) and phase margins (GPM) in the output channels are*[1]*:*

GGM: $[0, \infty)$
GPM: $[-90, +90]$ *deg.*

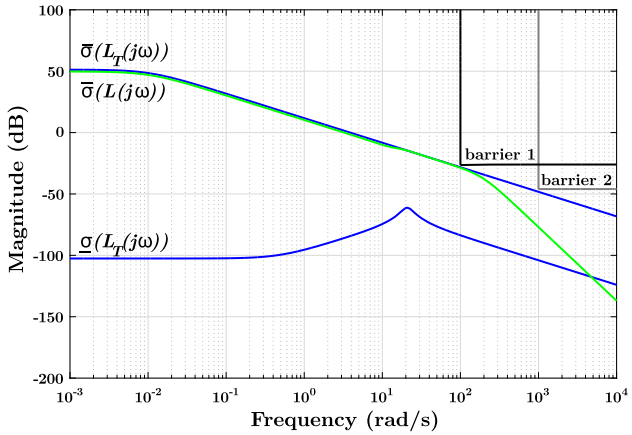

Fig. 3 Maximum and minimum singular values of the target loop, maximum singular value of the achieved loop, and high-frequency noise rejection barriers

Hence, if K_f is designed according to the Lyapunov Filter procedure not only $(A - K_f C)$ Hurwitz is ensured, but also that arbitrary attenuations on the outputs channels will not compromise stability. The free parameters were chosen as $Q = 0.023 \times I$, $R = 0.29 \times I$, resulting in

$$P = \begin{bmatrix} 1.1216 & 0.0002 & -0.0115 & 0.0056 \\ 0.0002 & 0.0018 & -0.0056 & -0.0115 \\ -0.0115 & -0.0056 & 0.0613 & 0.1983 \\ 0.0056 & -0.0115 & 0.1983 & 0.7226 \end{bmatrix} \tag{17}$$

$$K_f = \begin{bmatrix} 3.8676 & 0.0007 & -0.0397 & 0.0192 \\ 0.0007 & 0.0063 & -0.0192 & -0.0397 \end{bmatrix}^T. \tag{18}$$

As shown in Fig. 3, the singular values of the target loop transfer function do not violate the sensor noise rejection barriers. Moreover, $\overline{\sigma}(L_T(j\omega))$ assumes values close to 50 dB below 10^{-2} rad/s and presents a cutoff frequency of approximately 3.3 rad/s, whereas $\underline{\sigma}(L_T(j\omega))$ has magnitude lower than -50 dB in the entire frequency spectrum. Although the low magnitude values may suggest low performance prima facie, the reference signals which are to be applied to the closed-loop system have a specific direction as stated in the design requirements. By avoiding the minimum singular value direction, the obtained reference tracking performance is satisfactory as confirmed by the experimental results.

[1] The concept of multivariable stability margins is defined in Lehtomaki et al. (1981).

3.2 Loop Transfer Recovery

Several controller structures for LTR are available in the literature (Prakash 1990b; Saberi et al. 1993; Pereira and Kienitz 2014). Herein, we consider the following output-feedback controller for loop recovery (Athans 1986)

$$\dot{z}(t) = Az(t) + Bu(t) + K_f[-e(t) - Cz(t)] \tag{19}$$

$$u(t) = -K_r z(t) \tag{20}$$

where $z(t)$ is the controller internal state, $e(t)$ is the error signal, $u(t)$ is the control input, $\{A, B, C\}$ are the same matrices from the plant nominal model, K_f is the filter gain calculated in the TFL phase, and K_r is the regulator gain which is yet to be determined. Next, the LTR procedure described in Prakash (1990b) for PRO designs is employed.

Given a scalar parameter $q \in \mathbb{R}_{>0}$ and $V \in \mathbb{R}^{p\times p}$, $V \succ 0$, Q is calculated as

$$Q = q^2 C^T C. \tag{21}$$

For $R \in \mathbb{R}^{p\times p}$, $R \succ 0$, the algebraic Riccati equation

$$PA + A^T P + Q - PBR^{-1}B^T P = 0 \tag{22}$$

is solved for P. The regulator gain is then given by

$$K_r = R^{-1}B^T P. \tag{23}$$

It is guaranteed that the error between the target dynamics $L_T(s)$ and the obtained loop transfer $L(s)$ will converge to zero as the recovery parameter q is increased (Doyle and Stein 1981). More specifically,

$$\lim_{q\to\infty} L(s) = L_T(s) \tag{24}$$

holds pointwise in the complex domain, where $L(s) = G(s)K(s)$.

The design parameters were chosen as $R = 10^{-4}$ and $q = 150$, yielding

$$P = \begin{bmatrix} 1094.61 & -853.45 & 37.1437 & -36.2734 \\ -853.45 & 962.8540 & -27.9844 & 28.4032 \\ 37.1437 & -27.9844 & 3.91077 & -3.87547 \\ -36.2734 & 28.4032 & -3.87547 & 3.8490 \end{bmatrix} \tag{25}$$

$$K_r = 10^4 \begin{bmatrix} 1.5000 & 0.7218 & 0.0608 & -0.0456 \end{bmatrix}. \tag{26}$$

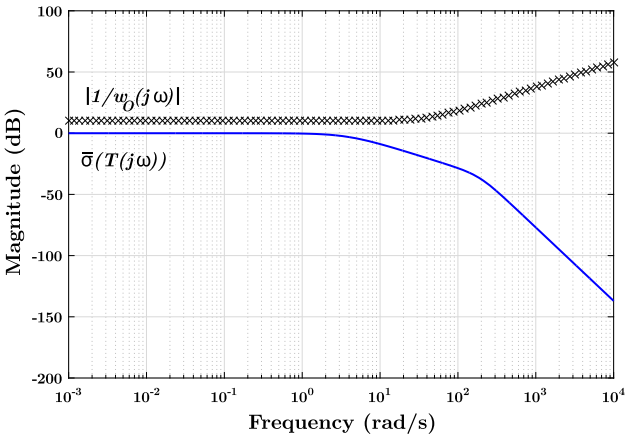

Fig. 4 Robust stability verification: output multiplicative uncertainty weight inverse and complementary sensitivity function maximum singular value

The obtained controller transfer function matrix was

$$K(s) = \left[\frac{57985\,(s+11.29)\,(s^2+7.349s+435.6)}{(s^2+13.08s+248.6)\,(s^2+272.6s+37320)} \cdots \right. \\ \left. \cdots \frac{61.629\,(s+19.2)\,(s+7.401)\,(s-2.354)}{(s^2+13.08s+248.6)\,(s^2+272.6s+37320)}\right] \tag{27}$$

with poles located at $-111.40 \pm j112.17$ and $-6.51 \pm j14.36$, thus, stable. Clearly, an order reduction technique could be employed in case the controller was to be implemented in a low processing power hardware platform.

The quality of the recovery procedure can be assessed in Fig. 3, where both maximum singular values were considered sufficiently matched up to 100 rad/s. On the other hand, as a consequence of the system underactuation, the minimum singular value was not recovered and $\underline{\sigma}(L(j\omega))$ is not shown due to its low magnitude.

Robust stability in the presence of the output multiplicative uncertainties given by (10) and (11) is attained if (Athans 1986; da Cruz 1996)

$$\overline{\sigma}(T(j\omega)) < \frac{1}{|w_0(j\omega)|}, \quad \forall\omega. \tag{28}$$

This condition is verified in Fig. 4 since the maximum singular value of the complementary sensitivity function does not exceed the output multiplicative uncertainty weight inverse module.

4 Experimental Results

Experiments were conducted with the system starting at the origin. A ramp with slope 60 cm/s was applied as the active

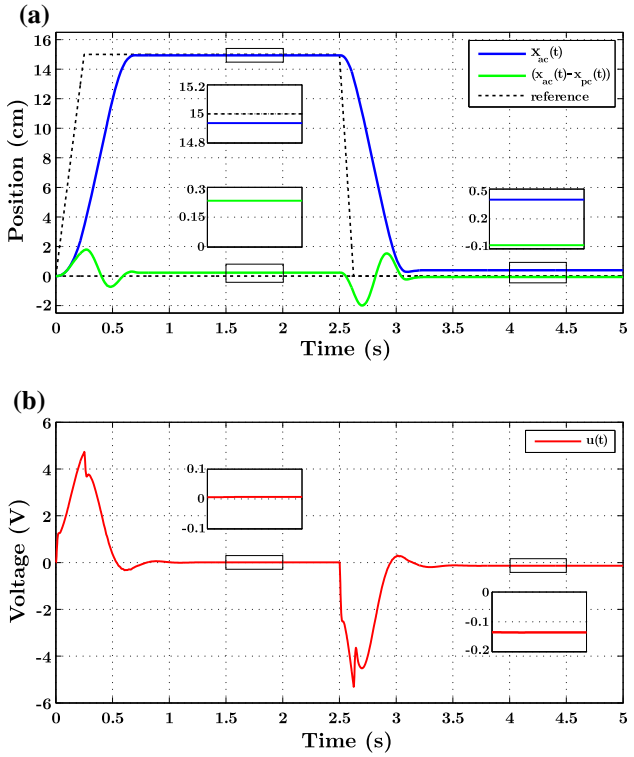

Fig. 5 Experimental results in normal operation: **a** active cart position and spring deformation, **b** DC motor voltage

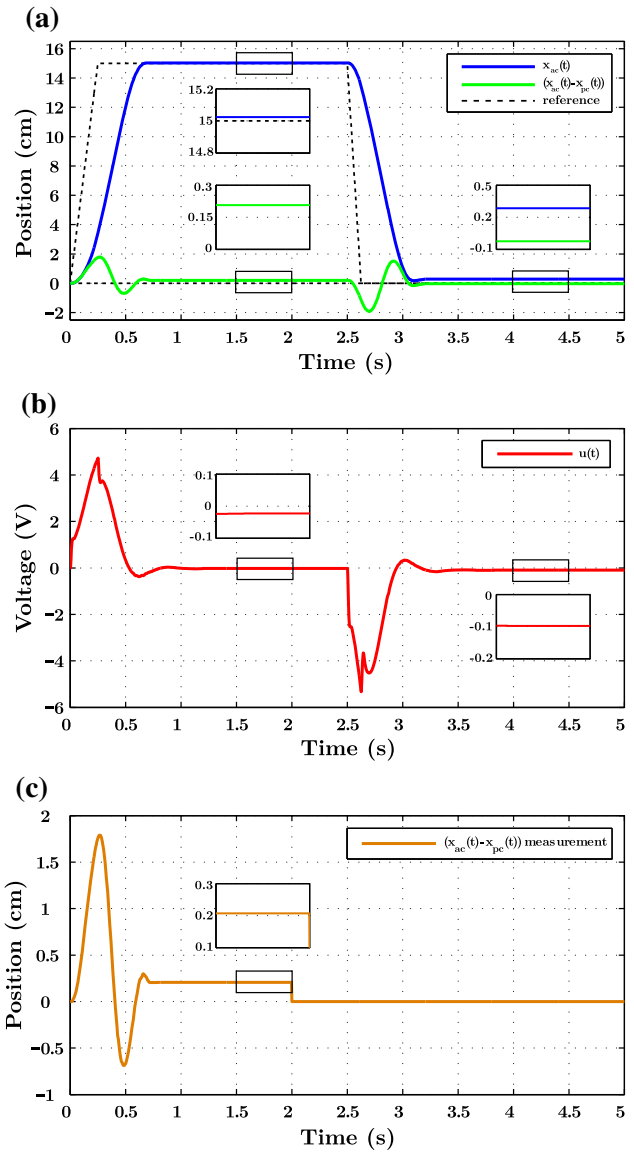

Fig. 6 Experimental results with sensor fault at 2 s: **a** active cart position and spring deformation, **b** DC motor voltage, **c** spring deformation measurement

cart reference until a 15 cm platoon was reached (first movement); at 2 s, the reference was brought back to the origin with a ramp of slope -120 cm/s (second movement). The spring deformation reference was kept at zero during the whole maneuver. Moreover, the input signal was bounded to $[-6, +6]$ V in accordance with the manufacturer's specifications. The obtained reference tracking results and demanded control effort are shown in Fig. 5.

In the fist movement, the first output reached 13.5 cm in 0.558 s and presented a steady-state error of -0.060 cm since the internal control loop moved the original pole from the origin, whereas in the second movement, the first output reached 1.5 cm in 0.490 s with a final error of 0.393 cm due to the nonlinear effects of dry friction (de Wit et al. 1993; Urbakh et al. 2004), which was approximated by viscous friction in the modeling process. The spring was subjected to deformation peaks of 1.793 cm and -1.993 cm in the first and second movements, respectively. During the whole maneuver, the control input remained within its predefined bounds, thus avoiding any saturation. The final DC motor voltage was -0.135 V, still not high enough to reach the threshold of motion and correct the outputs deviations with respect to the references.

In a second experiment, the same previously described reference signals were employed, but an abrupt sensor fault in the second output channel was considered at 2 s. Hence, the first movement was accomplished by the linear positioning system with both sensors, while the second movement was carried out with only the active cart position sensor as shown in Fig. 6. The first output reached 13.5 cm in 0.553 s and presented a steady-state error of 0.020 cm in accordance with the first experiment. However, steady-state error on the second movement was reduced to 0.284 cm and the final DC motor voltage to -0.098 V, since the controller is no longer fed with the error from the second output. Regardless, closed-loop stability was preserved.

The pre-stabilization loop contribution to the overall control signal as described in Sect. 2.1 is not significant. Indeed, the feedback gain ϵ could be made arbitrarily small and the

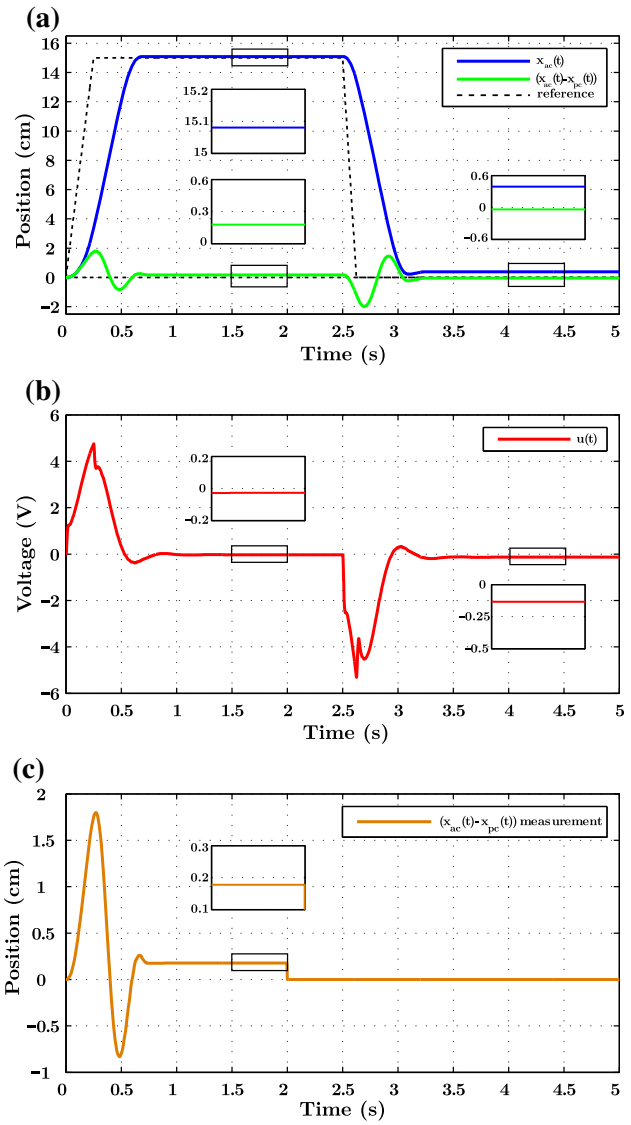

Fig. 7 Experimental results with no pre-stabilization loop and with sensor fault at 2 s: **a** active cart position and spring deformation, **b** DC motor voltage, **c** spring deformation measurement

Lyapunov Filter restrictions would still be satisfied. Consequently, it can be argued that its implementation is immaterial in practice. A necessary condition for being able to neglect the internal loop during operation is $Re\{\lambda_i(A)\} \leq 0, i = 1, \ldots, n$ since, if at least one eigenvalue λ_i of the state matrix has a positive real component, then there exists a minimum feedback gain different from zero necessary to relocate that system pole to the open left half-plane.

In view of the above observations, the internal loop was not implemented in the last experiment and the plant was solely controlled by the TFL/LTR compensator. A sensor fault was also considered at 2 s, and the results are shown in Fig. 7. Although the obtained response on the first movement was qualitatively similar to the one presented in Fig. 6, the active cart position exhibited slightly higher steady-state error when returning to the origin due to absence of the internal loop. Also, no control saturation or instability occurred.

Despite being a passive fault-tolerant technique, the proposed methodology attained reference tracking results for the active cart comparable to the ones reported in Junior et al. (2016), where a robust model predictive control (RMPC) formulation was chosen to tackle exactly the same system. Regarding spring deformation, the RMPC approach considered by the authors was capable of further reducing its compression and elongation, satisfying a constraint $|x_{\mathrm{ac}}(t) - x_{\mathrm{pc}}(t)| < 1, \forall t > 0$. Nonetheless, while the TFL/LTR controller is a straightforward linear output-feedback structure, the solution proposed in Junior et al. (2016) requires all states and relies on the online solution of a semidefinite optimization problem at each sampling period.

5 Concluding Remarks

A Lyapunov filter-based TFL/LTR controller was designed for an underactuated linear positioning mechanism. Robustness against parameters uncertainties and abrupt sensor faults was attained. It was shown that the Lyapunov filter (linear Lyapunov regulator) technique can still be applied to open-loop unstable systems if a pre-stabilization loop is designed. This internal feedback compensator must employ as few sensors (actuators) as possible, since fault tolerance will be guaranteed in the remaining channels. In special cases such as the one considered in this paper, the internal loop can be dispensed in practice and the TFL/LTR compensator can be directly applied to the plant. A necessary condition for this end was given.

One drawback of the presented method, and of most loop shaping techniques, is the difficulty of constructing target loops for specific time domain requirements, since the designer has to rely on the manual adjustment of the free parameters in a trial and error fashion. Finally, pre-stabilization of the linear positioning system was accomplished by means of a simple proportional feedback loop. However, this same task could be fulfilled in numerous other ways. The benefits of choosing one approach or another to the overall system performance and robustness are to be explored in the future.

Acknowledgements This work was supported by the Brazilian agencies CAPES (scholarship), CNPq (Grant #309331/2015-3) and FAPESP (Grant #11/17610-0).

References

Abbas-Turki, M., Duc, G., Clement, B., & Theodoulis, S. (2007). Robust gain scheduled control of a space launcher by introducing

LQG/LTR ideas in the NCF robust stabilisation problem. In *Proceedings of conference on decision and control* (pp. 2393–2398).
Alwi, H., Edwards, C., & Tan, C. P. (2011). *Fault detection and fault-tolerant control using sliding modes*. New York: Springer.
Arab-Alibeik, H., & Setayeshi, S. (2003). Improved temperature control of a PWR nuclear reactor using an LQG/LTR based controller. *IEEE Transactions on Nuclear Science*, *50*(1), 211–218.
Athans, M. (1986). A tutorial on the LQG/LTR method. In *Proceedings of American control conference* (pp. 1289–1296).
Calise, A. J., & Yucelen, T. (2012). Adaptive loop transfer recovery. *Journal of Guidance, Control, and Dynamics*, *35*(3), 807–815.
Chen, M. S., & Chen, C. C. (2008). Output feedback control of bilinear systems via a bilinear LTR observer. *IEEE Transactions on Automatic Control*, *53*(2), 617–621.
da Cruz, J. J. (1996). Controle robusto multivariável: O método LQG/LTR. Editora da Universidade de São Paulo.
da Silva, D. L., de Paula, C. F., & Ferreira, L. H. (2014). A new look at the target feedback loop parameterization for $\mathcal{H}_\infty$/LTR control. *Journal of Control, Automation and Electrical Systems*, *25*(4), 389–399.
de Moraes, A. T., & Kienitz, K. H. (2017). Robust control of an industrial pilot plant. *IEEE Latin America Transactions*, *15*(9), 1613–1620.
de Paula, C. F., & Ferreira, L. H. C. (2011). An easy-to-use $\mathcal{H}_\infty$/LTR control solution with mixed-sensitivity properties. *IEEE Transactions on Automatic Control*, *56*(7), 1709–1713.
de Wit, C. C., Olsson, H., Åström, K. J., & Lischinsky, P. (1993). A new model for control of systems with friction. *IEEE Transactions on Automatic Control*, *40*(3), 419–425.
Doyle, J. (1978). Guaranteed margins for LQG regulators. *IEEE Transactions on Automatic Control*, *23*(4), 756–757.
Doyle, J., & Stein, G. (1979). Robustness with observers. *IEEE Transactions on Automatic Control*, *24*(4), 607–611.
Doyle, J., & Stein, G. (1981). Multivariable feedback design: Concepts for a classical/modern synthesis. *IEEE Transactions on Automatic Control*, *26*(1), 4–16.
George, J. (2014). On adaptive loop transfer recovery using kalman filter-based disturbance accommodating control. *IET Control Theory & Applications*, *8*(4), 267–276.
Guaracy, F. H., Ferreira, L. H., & Pinheiro, C. A. (2015a). The discrete-time controller for the $\mathcal{H}_\infty$/LTR problem with mixed-sensitivity properties. *Automatica*, *58*, 28–31.
Guaracy, F. H., da Silva, D. L., & Ferreira, L. H. (2015b). On the properties of augmented open-loop stable plants using LQG/LTR control. *IEEE Transactions on Automatic Control*, *60*(8), 2172–2176.
Ishihara, T., & Guo, H. J. (2008). LTR design of disturbance cancellation integral controllers for time-delay plants. *International Journal of Control*, *81*(7), 1027–1034.
Junior, J. R. C., Afonso, R. J. M., Galvão, R. K. H., & Assunção, E. (2016). Robust model predictive control of a benchmark electromechanical system. *Journal of Control, Automation and Electrical Systems*, *27*(2), 119–131.
Kwakernaak, H. (1969). Optimal low-sensitivity linear feedback systems. *Automatica*, *5*(3), 279–285.
Lavretsky, E. (2012). Adaptive output feedback design using asymptotic properties of LQG/LTR controllers. *IEEE Transactions on Automatic Control*, *57*(6), 1587–1591.
Lehtomaki, N., Sandell, N. J. A. M., & Athans, M. (1981). Robustness results in linear-quadratic gaussian based multivariable control designs. *IEEE Transactions on Automatic Control*, *26*(1), 75–93.
Maciejowski, J. (1985). Asymptotic recovery for discrete-time systems. *IEEE Transactions on Automatic Control*, *30*(6), 602–605.
Maddalena, E. T. (2017). Fault-tolerant control using the TFL/LTR design procedure. Master's thesis, Instituto Tecnológico de Aeronáutica.
Maddalena, E. T., & Kienitz, K. H. (2017). Fault-tolerant control of an underactuated system using a generalization of the LQG/LTR method. In *Proceedings of 24th international congress of mechanical engineering* (pp. 1–8).
Niemann, H., & Stoustrup, J. (2003). Controller reconfiguration based on LTR design. In *Proceedings of 42nd conference on decision and control* (pp. 2453–2458).
Pereira, R. L., & Kienitz, K. H. (2014). Robust controllers using generalizations of the LQG/LTR method. *Journal of Control, Automation and Electrical Systems*, *25*(3), 273–282.
Pinto, V. P., Campos, J. C. T., dos Reis, L. L. N., Jacobina, C. B., & Rocha, N. (2011). Robustness and performance analysis for the linear quadratic gaussian/loop transfer recovery with integral action controller applied to doubly fed induction generators in wind energy conversion systems. *Electric Power Components and Systems*, *40*(2), 131–146.
Prakash, R. (1990a). Target feedback loop/loop transfer recovery (TFL/LTR) robust control design procedures. In *Proceedings of 29th conference on decision and control* (pp. 1203–1209).
Prakash, R. (1990b). Target feedback loop/loop transfer recovery (TFL/LTR) robust control system design. PhD thesis, University of Missouri-Rolla.
Prakash, R. (1992). Robust control of an induction motor drive with lyapunov filter and linear quadratic regulator. In *Proceedings of American control conference* (pp. 1725–1731).
Quanser Consulting. (2012). *Linear flexible joint cart-workbook*. Markham, ON: Quanser Consulting.
Ravanbod, L., Noll, D., & Apkarian, P. (2012). An extension of the linear quadratic gaussian-loop transfer recovery procedure. *IET Control Theory & Applications*, *6*(14), 2269–2278.
Saberi, A., Chen, B. M., & Sannuti, P. (1991a). Theory of LTR for non-minimum phase systems, recoverable target loops, and recovery in a subspace Part 1. Analysis. *International Journal of Control*, *53*(5), 1067–1115.
Saberi, A., Chen, B. M., & Sannuti, P. (1991b). Theory of LTR for non-minimum phase systems, recoverable target loops, and recovery in a subspace Part 2. Design. *International Journal of Control*, *53*(5), 1117–1160.
Saberi, A., Peddapullaiah, S., & Chen, B. M. (1993). *Loop transfer recovery: Analysis and design*. New York: Springer.
Skogestad, S., & Postlethwaite, I. (2001). *Multivarible feedback control: Analysis and design*. New York: Wiley.
Stein, G., & Athans, M. (1987). The LQG/LTR procedure for multivariable feedback control design. *IEEE Transactions on Automatic Control*, *32*(2), 105–114.
Urbakh, M., Klafter, J., Gourdon, D., & Israelachvili, J. (2004). The nonlinear nature of friction. *Nature*, *430*(6999), 525–528.
Zarei, J., Montazeri, A., Motlagh, M. R. J., & Poshtan, J. (2007). Design and comparison of LQG/LTR and $\mathcal{H}_\infty$ controllers for a VSTOL flight control system. *Journal of the Franklin Institute*, *344*(5), 577–594.
Zhang, Z., & Freudenberg, J. S. (1990). Loop transfer recovery for non-minimum phase plants. *IEEE Transactions on Automatic Control*, *35*(5), 547–553.
Zolotas, A. C., Chaudhuri, B., Jaimoukha, I. M., & Korba, P. (2007). A study on LQG/LTR control for damping inter-area oscillations in power systems. *IEEE Transactions on Control Systems Technology*, *15*(1), 151–160.